RESEARCH ARTICLE

Circulating Tumor DNA Genomics Correlate with Resistance to Abiraterone and Enzalutamide in Prostate Cancer

Matti Annala[1,2], Gillian Vandekerkhove[1], Daniel Khalaf[3], Sinja Taavitsainen[2], Kevin Beja[1], Evan W. Warner[1], Katherine Sunderland[3], Christian Kollmannsberger[3], Bernhard J. Eigl[3], Daygen Finch[4], Conrad D. Oja[5], Joanna Vergidis[6], Muhammad Zulfiqar[7], Arun A. Azad[8], Matti Nykter[2], Martin E. Gleave[1], Alexander W. Wyatt[1], and Kim N. Chi[1,3]

ABSTRACT

Primary resistance to androgen receptor (AR)–directed therapies in metastatic castration-resistant prostate cancer (mCRPC) is poorly understood. We randomized 202 patients with treatment-naïve mCRPC to abiraterone or enzalutamide and performed whole-exome and deep targeted 72-gene sequencing of plasma cell-free DNA prior to therapy. For these agents, which have never been directly compared, time to progression was similar. Defects in *BRCA2* and *ATM* were strongly associated with poor clinical outcomes independently of clinical prognostic factors and circulating tumor DNA abundance. Somatic alterations in *TP53*, previously linked to reduced tumor dependency on AR signaling, were also independently associated with rapid resistance. Although detection of *AR* amplifications did not outperform standard prognostic biomarkers, *AR* gene structural rearrangements truncating the ligand binding domain were identified in several patients with primary resistance. These findings establish genomic drivers of resistance to first-line AR-directed therapy in mCRPC and identify potential minimally invasive biomarkers.

SIGNIFICANCE: Leveraging plasma specimens collected in a large randomized phase II trial, we report the relative impact of common circulating tumor DNA alterations on patient response to the most widely used therapies for advanced prostate cancer. Our findings suggest that liquid biopsy analysis can guide the use of AR-targeted therapy in general practice. *Cancer Discov; 8(4); 444–57. ©2018 AACR.*

See related commentary by Jayaram et al., p. 392.

INTRODUCTION

Recent years have seen a dramatic shift in the treatment of metastatic castration-resistant prostate cancer (mCRPC) with the potent androgen receptor (AR)–directed agents abiraterone acetate and enzalutamide currently indicated as first-line therapy (1, 2). Enzalutamide is a direct AR antagonist, whereas abiraterone depletes endogenous AR ligands through inhibition of CYP17-mediated steroidogenesis. These agents have not been directly compared in a clinical trial, and predictive

[1]Vancouver Prostate Centre, Department of Urologic Sciences, University of British Columbia, Vancouver, British Columbia, Canada. [2]Faculty of Medicine and Life Sciences and Biomeditech Institute, University of Tampere, Tampere, Finland. [3]British Columbia Cancer Agency, Vancouver Centre, Vancouver, British Columbia, Canada. [4]British Columbia Cancer Agency, Southern Interior Centre, Kelowna, British Columbia, Canada. [5]British Columbia Cancer Agency, Fraser Valley Centre, Vancouver, British Columbia, Canada. [6]British Columbia Cancer Agency, Vancouver Island Centre, Victoria, British Columbia, Canada. [7]British Columbia Cancer Agency, Abbotsford Centre, Vancouver, British Columbia, Canada. [8]Monash University, Monash, Australia.

Note: Supplementary data for this article are available at Cancer Discovery Online (http://cancerdiscovery.aacrjournals.org/).

A.W. Wyatt and K.N. Chi share senior authorship of this article.

Corresponding Authors: Alexander W. Wyatt, University of British Columbia, 2660 Oak Street, Vancouver, BC V6H 3Z6, Canada. Phone: 604-364-1940; Fax: 604-675-8019; E-mail: awyatt@prostatecentre.com; and K.N. Chi, Vancouver Prostate Centre, Department of Urologic Sciences, University of British Columbia, 2660 Oak Street, Vancouver, BC V6H 3Z6, Canada. Phone: 604-875-4818; Fax: 604-875-5654; E-mail: kchi@bccancer.bc.ca

doi: 10.1158/2159-8290.CD-17-0937

biomarkers for the 20% of first-line patients who exhibit primary or rapidly acquired resistance are lacking.

The abundance of plasma circulating tumor DNA (ctDNA) in patients with mCRPC has invigorated biomarker development previously hampered by the impracticality of routinely sampling osseous metastatic tissue. Using so-called liquid biopsies, primary and acquired resistance to AR-targeted therapy has been linked to amplification or mutation of the *AR* gene (3–7) and also to the expression (in circulating tumor cells) of truncated *AR* splice variants that display ligand-independent activity (8, 9). The impact of these biomarkers in patients with first-line mCRPC has not been adequately studied, and it is unclear whether the detection of *AR* alterations in patient ctDNA can outperform standard clinical prognostic factors. The relative impact of other genomic alterations on resistance and patient outcomes also remains to be elucidated in standardized clinical cohorts.

Here, we applied a combination of whole-exome and/or deep targeted sequencing to perform an opportunistic exploratory analysis of plasma-derived cell-free DNA (cfDNA) samples from 202 patients with first-line mCRPC enrolled in a randomized phase II trial of abiraterone versus enzalutamide (NCT02125357). We propose new genomic drivers of resistance to AR-directed therapy and show that cfDNA sequencing provides a practical means for assaying these potential treatment-guiding biomarkers.

RESULTS

Enzalutamide Elicits Superior PSA Responses but No Difference in Progression-Free Survival

Two hundred two patients with treatment-naïve mCRPC were randomized to abiraterone plus prednisone ($n = 101$) or enzalutamide ($n = 101$) between November 2014 and October 2016 (Fig. 1A; Supplementary Table S1). Median follow-up at time of analysis was 12.9 months (range, 0–32.1 months). Baseline characteristics were similar between arms, except for age (Table 1). Time to progression [TTP; first of confirmed prostate-specific antigen (PSA) progression, clinical or radiologic progression, or death from disease] did not differ between arms (median 7.5 vs. 7.5 months, HR = 0.82 for enzalutamide; 95% CI, 0.58–1.16, $P = 0.27$, univariate; Fig. 1B). However, enzalutamide achieved greater PSA responses than abiraterone, including a higher proportion of patients with PSA decline ≥ 50% from baseline within 12 weeks (75% vs. 54%, $P = 0.004$, Fisher exact test), and a lower proportion of patients with rising PSA as best response within the first 12 weeks of therapy (9% vs. 20%, $P = 0.046$, Fisher exact test; Fig. 1C).

ctDNA Fraction Is Associated with Tumor Burden and Clinical Outcomes

The majority of patients with mCRPC studied to date have plasma ctDNA fractions (ctDNA%, the proportion of

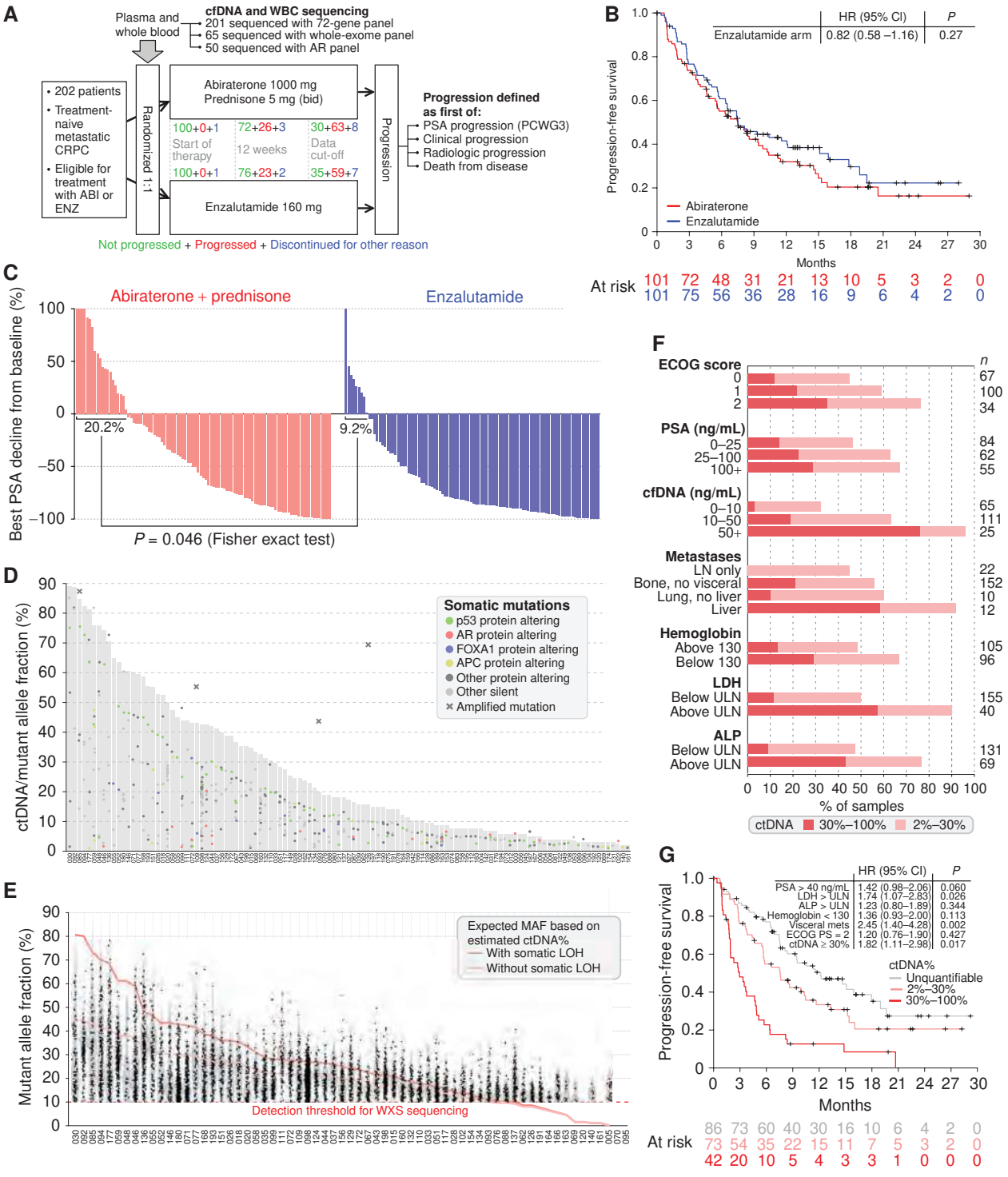

Figure 1. Time to progression on enzalutamide or abiraterone therapy and relationship with baseline ctDNA fraction. **A,** Study design and clinical endpoints. Number of patients and their status at three time points is shown for each arm. **B,** Kaplan–Meier estimate of progression-free survival in the abiraterone and enzalutamide arms. Univariate Cox proportional hazard regression is shown in the top right corner. **C,** Best PSA decline during first 12 weeks of therapy. Complete lack of PSA response was more common in the abiraterone arm. **D,** Estimated ctDNA% (gray bars) in the 115 cfDNA samples with detectable ctDNA based on somatic mutations (dots). **E,** Allele fractions of somatic mutations (black dots) detected in the 65 cfDNA samples subjected to whole-exome sequencing. Kernel density estimates of the allele fractions are shown in gray. Patients are sorted by ctDNA% (estimated from the 72-gene panel). Red lines indicate expected allele fractions of somatic mutations with and without somatic LOH. **F,** Fractions of patients with ctDNA > 30% and ctDNA between 2% and 30%, in various clinical subgroups. Note that the "lymph node only" subgroup of metastatic pattern excludes patients with metastases to any "other" site (e.g., bladder base, skin). **G,** Kaplan–Meier survival curves for patients stratified into three groups based on ctDNA%. Result of multivariate Cox proportional hazards regression is shown in the top right corner. ABI, abiraterone; ALP, alkaline phosphatase; ECOG, Eastern Cooperative Oncology Group; ENZ, enzalutamide; HR, hazard ratio; LDH, lactate dehydrogenase; LN, lymph node; LOH, loss of heterozygosity; MAF, mutant allele fraction; PCWG3, Prostate Cancer Clinical Trials Working Group 3; ULN, upper limit of normal; WBC, white blood cell; WXS, whole-exome sequencing.

Table 1. Patient characteristics at baseline

	All ($n = 202$)	ABI arm ($n = 101$)	ENZ arm ($n = 101$)	*P* value
Age	75.3 (49.3–94.1)	72.9 (51.3–93.3)	77.6 (49.3–94.1)	0.025
PSA (ng/mL)	36.1 (1.7–2817)	35.0 (2.2–2817)	37.0 (1.7–1060)	0.286
ALP (ULN)	0.81 (0.29–47.8)	0.82 (0.29–12.5)	0.75 (0.30–47.8)	0.771
LDH (ULN)	0.79 (0.31–12.9)	0.79 (0.37–4.0)	0.80 (0.31–12.9)	0.332
Hemoglobin (g/L)	130 (89–165)	130 (89–155)	130 (89–165)	0.988
ECOG PS 0–1	168 (83.2%)	89 (88.1%)	79 (78.2%)	0.090
Bone metastases	169 (83.7%)	86 (85.1%)	83 (82.2%)	0.704
Lung metastases	15 (7.4%)	7 (6.9%)	8 (7.9%)	1.000
Liver metastases	12 (5.9%)	5 (5.0%)	7 (6.9%)	0.767
cfDNA (ng/mL plasma)	13.0 (1.5–3871)	12.4 (1.5–258)	13.3 (1.5–3871)	0.424
ctDNA >2%	115 (56.9%)	56 (55.4%)	59 (58.4%)	0.839

NOTE: Alkaline phosphatase (ALP) and lactate dehydrogenase (LDH) levels are reported relative to upper limit of normal (ULN).

Abbreviations: ABI, abiraterone; ECOG PS, Eastern Cooperative Oncology Group performance status; ENZ, enzalutamide; PSA, prostate-specific antigen.

tumor-derived cfDNA) above 2% (3, 5, 6, 10, 11). cfDNA sequencing involves a tradeoff between cost, genome coverage, and sensitivity to low ctDNA%. We used a targeted sequencing strategy capturing all exons of 72 mCRPC driver genes (Supplementary Table S2). We have previously demonstrated that this approach identifies over 90% of somatic mutations present in matched metastatic tissue in patients with ctDNA > 2% (11). Consistent with this result, tumor DNA spike-in experiments suggested greater than 90% sensitivity for somatic variants with an allele fraction above 3.5% (Supplementary Fig. S1). Copy-number changes were detected at ctDNA fractions above ~30%, although exact sensitivity varied depending on the nature of the alteration (e.g., monoallelic versus biallelic deletion; Supplementary Fig. S2).

Baseline cfDNA samples from 201 patients (one sample failed cfDNA extraction) were sequenced to a median depth of 688× (Supplementary Figs. S3–S4). ctDNA fraction was quantifiable in 115 of 201 (57%) cfDNA samples based on the presence of detectable somatic mutations (Fig. 1D; Supplementary Table S3). Two additional patients had AR amplifications but no somatic mutations above our detection threshold (Supplementary Fig. S5). Estimated ctDNA% in the 115 patients ranged between 2% and 89% (median 17%). The highest ctDNA% (89%) was observed in patient 030, supported by two somatic mutations with loss of heterozygosity (LOH; Supplementary Table S3). The sample yielded 175 ng cfDNA/mL plasma, 13-fold more than the cohort median.

To confirm estimated ctDNA fractions, 65 baseline cfDNA and germline pairs were subjected to whole-exome sequencing at a median depth of 163× (Supplementary Fig. S6 and Supplementary Table S1). All somatic mutations detected with the 72-gene panel were confirmed by exome sequencing, and allele fractions were highly concordant ($R^2 = 0.90$; Supplementary Fig. S7). Allele fractions of somatic mutations outside the 72-gene panel were also consistent with estimated ctDNA% (Fig. 1E).

Leveraging the approximate ctDNA fraction where single copy-number changes in individual genes are detected, we subdivided patients into three classes: high ctDNA (30%–100%), low ctDNA (2%–30%), and undetectable ctDNA (<2%). High ctDNA fraction was associated with clinical markers of tumor burden, including higher plasma concentrations of cfDNA, PSA, lactate dehydrogenase (LDH), and alkaline phosphatase (ALP; Fig. 1F; Supplementary Fig. S8). Importantly, ctDNA% > 30% was strongly related to poor therapy response even after adjustment for clinical prognostic factors, suggesting that ctDNA% reflects aspects of tumor biology or disease volume that are not captured by typical clinical parameters (Fig. 1G; Table 2).

ctDNA Recapitulates the Somatic Landscape of mCRPC

A total of 457 somatic mutations (54% protein altering) were detected in the 115 samples with ctDNA above our detection threshold (Fig. 2; Supplementary Table S4). The most commonly mutated genes were *TP53* (56% of patients), *AR* (11%), *FOXA1* (10%), *APC* (10%), *PTEN* (10%), and *SPOP* (10%), in accordance with tissue-based CRPC studies (Supplementary Fig. S9; ref. 12). Although copy-number calling is challenging in patients with low ctDNA% (3, 10), the copy-number landscape in patients with ctDNA% > 30% was characteristic of mCRPC (13), including recurrent loss of the tumor suppressors *TP53, RB1,* and *PTEN* and amplification of the oncogenes *MYC* and *AR* (Fig. S2). Copy-number calls in mCRPC driver genes were concordant between the 72-gene panel and exome sequencing (Supplementary Fig. S7). Several genomic rearrangements affecting *TP53, PTEN, FOXA1, APC,* as well as ETS family genes were identified (Fig. 2; Supplementary Table S5), despite our exon-limited approach. Two patients exhibited an exceptionally high mutational burden in targeted sequencing (Fig. 2). Patient 098 (37.9 mutations/Mb) harbored biallelic somatic loss of mismatch repair genes

Table 2. Clinical and laboratory attributes and their association with time to progression and overall survival

			Time to progression			Overall survival		
Clinical marker	Subgroup	No. patients	Median (months)	HR (95% CI)	*P* value	Median (months)	HR (95% CI)	*P* value
ctDNA%	30–100	42	2.9	3.56 (2.28–5.57)	<0.001	10.1	12.92 (5.68–29.42)	<0.001
	2–30	73	7.5	1.54 (1.02–2.33)	0.040	20.1	4.38 (1.86–10.32)	<0.001
	2–100	115	5.4	2.05 (1.42–2.96)	<0.001	16.8	7.51 (3.41–16.57)	<0.001
	Unquantifiable	86	12.0	Ref	Ref	NR	Ref	Ref
PSA	≥40	93	6.4	1.50 (1.06–2.13)	0.022	16.7	3.87 (2.18–6.87)	<0.001
	<40	109	9.3	Ref	Ref	NR	Ref	Ref
Hemoglobin	<130	96	6.3	1.52 (1.08–2.16)	0.017	20.2	1.66 (0.99–2.78)	0.053
	≥130	106	9.3	Ref	Ref	NR	Ref	Ref
LDH	≥1 × ULN	40	2.8	2.83 (1.90–4.20)	<0.001	11.1	4.86 (2.87–8.22)	<0.001
	<1 × ULN	156	9.3	Ref	Ref	25.0	Ref	Ref
ALP	≥1 × ULN	69	4.7	1.95 (1.36–2.79)	<0.001	15.8	4.31 (2.53–7.35)	<0.001
	<1 × ULN	132	9.4	Ref	Ref	NR	Ref	Ref
Mets	Liver or lung	22	2.7	2.62 (1.58–4.36)	<0.001	9.5	5.28 (2.84–9.83)	<0.001
	Liver	12	2.1	3.81 (2.02–7.20)	<0.001	9.5	7.05 (3.30–15.07)	<0.001
	Lung	15	2.8	2.40 (1.31–4.39)	0.004	9.3	4.90 (2.35–10.18)	<0.001
	No visceral	175	8.3	Ref	Ref	25.0	Ref	Ref
ECOG PS	2	34	5.7	1.44 (0.92–2.25)	0.106	12.2	3.22 (1.85–5.60)	<0.001
	0–1	168	8.0	Ref	Ref	25.0	Ref	Ref
Age	≥75 years	102	8.3	0.76 (0.54–1.08)	0.121	20.6	1.14 (0.68–1.90)	0.618
	<75 years	100	6.5	Ref	Ref	NR	Ref	Ref

NOTE: Hazard ratios and *P* values were calculated using univariate Cox proportional hazards models, comparing each subgroup to its corresponding reference subgroup (labeled as "Ref").

Abbreviations: ECOG PS, Eastern Cooperative Oncology Group performance status; NR, not reached.

MSH2 and *MSH6*, plus a frameshift in *MLH1*. Whole-exome sequencing confirmed the high somatic mutation rate, and both panels showed a mutation signature consistent with mismatch repair deficiency (Supplementary Fig. S10). Patient 163 (16.8 mutations/Mb) carried a somatic *MSH2* frameshift, but low ctDNA% precluded LOH assessment. Both patients carried an *AR* H875Y mutation and no *AR* amplification (Fig. 2). Monoallelic deletion of mismatch repair genes was not associated with elevated mutation rates (Supplementary Fig. S10).

Specific Classes of Genomic Alteration Are Independently Associated with Poor Clinical Outcomes

To explore the interaction between common genomic alterations and clinical outcomes, we first catalogued deleterious alterations in major prostate cancer driver genes and pathways covered by our panel (Fig. 3A; Supplementary Table S6). The majority (67%) of patients with ctDNA above 2% had defects in two or more of these pathways (Supplementary Fig. S11). We observed established patterns of mutual exclusivity between molecular subtypes (e.g., *TP53* defects vs. *SPOP* missense mutations; $P = 0.008$, Fisher exact test). In univariate analysis of each alteration class, hazard ratios for TTP ranged between 1.00 and 6.14 (Table 3). We did not observe evidence for differential efficacy between abiraterone and enzalutamide within any genomic or clinical subgroup (Supplementary Fig. S12). Therefore, we merged the trial arms and performed a multivariate analysis for each individual gene or pathway, incorporating both clinical prognostic factors and presence of ctDNA as covariates. In this multivariate model, only deleterious alterations in homologous recombination repair genes (*BRCA2* or *ATM*) and *TP53* remained significantly associated with shorter TTP (Table 3; Fig. 3A–D; Supplementary Table S6).

The strongest prognostic association was observed for the 14 patients with truncating germline or somatic mutations in homologous recombination repair genes *BRCA2* or *ATM* (no truncating changes were detected in *BRCA1, PALB2,* or *FANCA* in the germline or somatic genomes). A remarkable 9 of 14 progressed before 12 weeks, suggesting a link with primary resistance (Fig. 3B; Supplementary Table S7). Four patients with germline mutations did not have ctDNA above our detection thresholds, but 8 of the remaining 10 patients with either germline or somatic BRCA2/ATM mutations had detectable LOH in ctDNA (Supplementary Fig. S13). The exceptions were two patients where LOH assessment was precluded due to low ctDNA fraction or somatic mutation subclonality

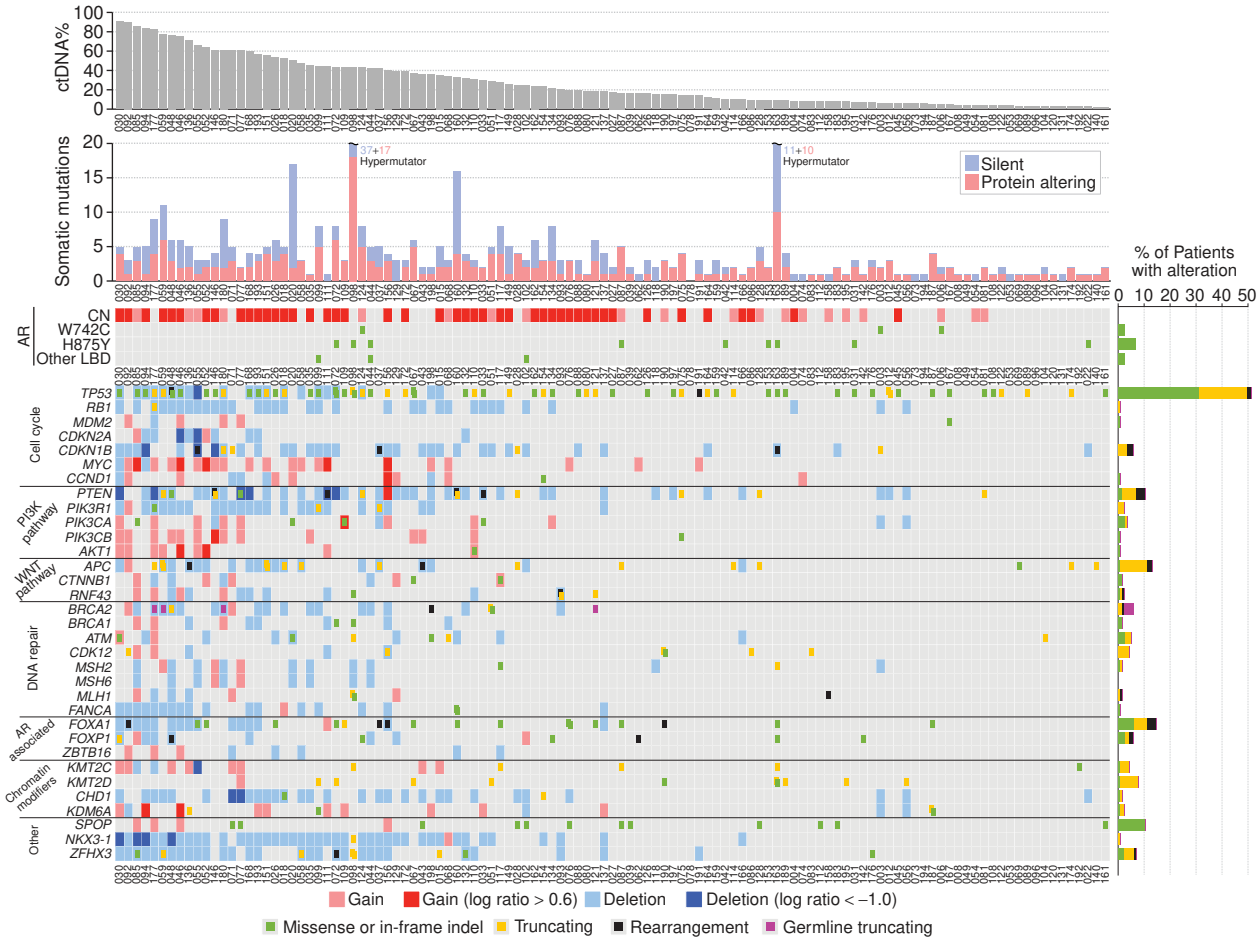

Figure 2. Genomic landscape of treatment-naïve mCRPC from targeted plasma cfDNA sequencing. Matrix of genomic alterations identified from cfDNA sequencing in the 115 patients with ctDNA above 2%. Patients are sorted by ctDNA% (top). Genes are grouped by pathway (34 genes shown). The number of detected somatic mutations is shown for each sample. Frequency of mutations and rearrangements in each gene is provided on the right. Two patients labeled as "hypermutator" exhibited evidence of mismatch-repair deficiency (see Supplementary Fig. S10).

(Supplementary Fig. S13). Importantly, we did not observe a significant association between detection of monoallelic *BRCA2/ATM* deletions (in the absence of truncating mutations) and shorter TTP in multivariate analysis (Table 3; Supplementary Table S6; Supplementary Fig. S13). This suggests that the independent prognostic association was confined to detection of a truncating mutation (note that we did not observe any biallelic *BRCA2/ATM* deletions in our cohort). There were only two patients with mismatch-repair gene mutations; however, we note that they also responded poorly to AR-targeted therapy: Patient 098 had no PSA response to abiraterone and patient 163 progressed on enzalutamide after 5.6 months.

Deleterious mutations, rearrangements, and deletions in *TP53* were identified in 65 of 115 (57%) patients with ctDNA above our detection threshold. Interestingly, 19 of 65 patients harbored two or more detectable defects in *TP53* and these patients exhibited even shorter TTP than patients with a single detectable defect (median 2.7 vs. 3.7 months, HR = 2.19; 95% CI, 1.18–4.08, $P = 0.013$, univariate; Fig. 3C; Table 3; Supplementary Table S6). Similar to *BRCA2/ATM* truncating mutations, somatic *TP53* defects were common in patients exhibiting primary resistance (Table 3; Supplementary Table S7). Indeed, among patients with ctDNA above our detection threshold who progressed prior to 12 weeks, 29 (81%) carried a somatic *TP53* mutation or deletion, and all but one of the remaining 7 patients had ctDNA% < 30% such that the presence of *TP53* deletions could not be ruled out. The detection of *TP53* alterations also demonstrated a strong association with poor overall survival, independent of clinical prognostic factors (Fig. 3D; Supplementary Table S8).

Importantly, although there was overlap between the subsets of patients harboring *BRCA2/ATM* truncating mutations and *TP53* defects, when all genomic and clinical variables were analyzed together in a single multivariate model, both *BRCA2/ATM* and *TP53* defects remained strongly and independently associated with patient outcomes (Supplementary Table S6). Similarly, the relationships between *BRCA2/ATM* or *TP53* defects and TTP were maintained even when

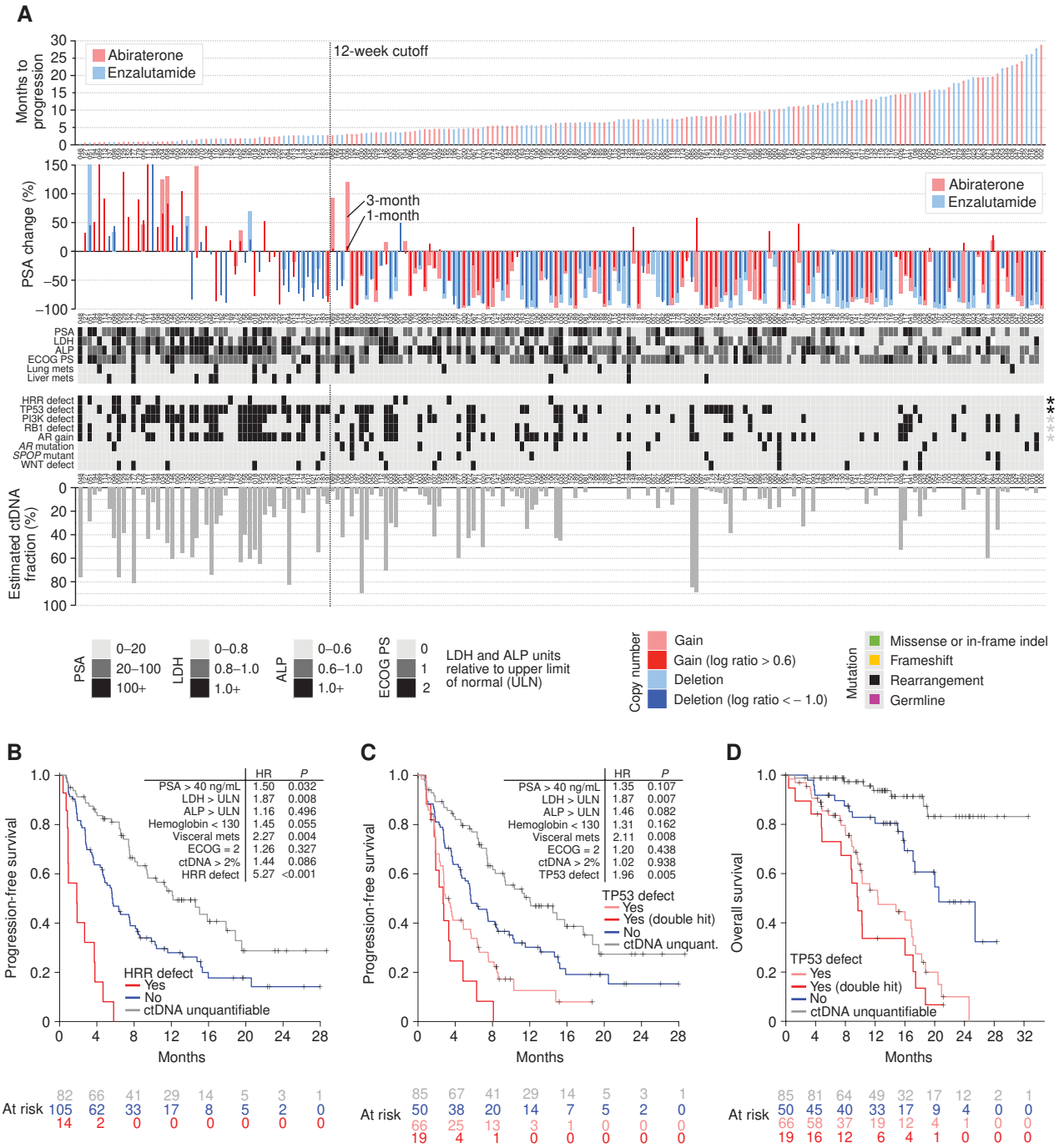

Figure 3. Genomic alterations in ctDNA and response to AR-targeted therapy. **A,** Swimmers plot of TTP on abiraterone (red) or enzalutamide (blue) showing matched PSA responses as well as major clinical and genomic factors for each patient. Arrowheads indicate right-censored TTP. Patients 120 and 199 were lost to follow-up immediately after study entry and are not shown. ctDNA% (estimated based on somatic mutations) is shown at bottom. Asterisks on the right side of genomic factors indicate statistical significance in multivariate (black) and univariate (gray) Cox proportional hazards regression (see Table 3). **B,** Kaplan–Meier plot of TTP in patients with and without homologous recombination repair (HRR) defects (defined here as truncating mutations in *BRCA2* or *ATM*), and patients without ctDNA above detection thresholds. Inset table shows multivariate analysis adjusting for clinical prognostic factors and ctDNA detection (see also Supplementary Table S6). **C,** Kaplan–Meier plot of TTP in patients with and without TP53 defects, and patients without ctDNA above detection thresholds. **D,** Kaplan–Meier plot of overall survival in patients with and without TP53 defects, and patients without ctDNA above detection thresholds.

Table 3. Individual genomic alterations and their association with TTP

Subgroup	Patients in subgroup	Median TTP (months)	% Patients with TTP < 12 weeks	Univariate Cox model		Multivariate Cox model	
				HR (95% CI)	*P* value	HR (95% CI)	*P* value
BRCA2/ATM truncating mutation	14	1.8	69.2%	6.14 (3.35–11.26)	<0.001	5.27 (2.79–9.95)	<0.001
BRCA2/ATM monoallelic deletion only	22	2.9	45.5%	2.58 (1.58–4.21)	<0.001	1.44 (0.82–2.53)	0.205
TP53 defect	66	3.3	48.4%	2.70 (1.86–3.91)	<0.001	1.96 (1.23–3.11)	0.005
TP53 defect (two or more)	19	2.7	62.5%	5.65 (3.14–10.17)	<0.001	3.40 (1.70–6.80)	<0.001
RB1 defect	37	3.6	41.7%	2.03 (1.36–3.04)	<0.001	1.39 (0.96–2.01)	0.081
AR gain	67	5.1	37.5%	2.05 (1.43–2.93)	<0.001	1.21 (0.77–1.91)	0.401
AR gain (CN ≥ 8)	31	2.7	51.7%	2.65 (1.68–4.19)	<0.001	1.48 (0.85–2.58)	0.164
AR gain (CN < 8)	36	6.3	25.7%	1.67 (1.07–2.62)	0.025	1.08 (0.63–1.85)	0.772
AR LBD mutation	14	6.2	7.1%	1.02 (0.53–1.95)	0.95	0.82 (0.40–1.68)	0.581
PI3K pathway defect	59	3.7	43.6%	2.45 (1.71–3.51)	<0.001	1.46 (0.94–2.27)	0.095
WNT pathway defect	16	4.8	33.3%	1.29 (0.71–2.34)	0.398	0.67 (0.35–1.28)	0.225
SPOP mutation	12	7.3	8.3%	1.00 (0.51–1.97)	1.00	0.43 (0.21–0.89)	0.022
ctDNA > 2%	115	5.4	31.8%	—	—	—	—
All patients	202	7.5	23.7%	—	—	—	—

NOTE: In each comparison, the analyses compare alteration-positive patients to those where no alteration in the gene/pathway was detected. Each genomic alteration is assessed individually in a multivariate model adjusting for significant clinical prognostic factors and the detection of ctDNA > 2% (Supplementary Table S6). A patient was considered alteration-positive for copy-number changes (e.g., AR gain), somatic rearrangements, and germline homologous recombination repair defects even if the patient had no detectable somatic mutations to quantify ctDNA fraction.

restricting analyses to high-risk patient subgroups based on clinical prognostic factors (Supplementary Fig. S14).

AR Amplification and Mutation Do Not Preclude Therapy Response

AR copy-number gain was identified in 65 of 115 (57%) baseline samples with ctDNA above detection thresholds (Fig. 4A). Although *AR* gain did not remain significantly associated with shorter TTP after adjustment for ctDNA presence and clinical prognostic factors, the hazard ratio in univariate analysis was 2.05 (95% CI, 1.43–2.93), similar to prior studies assessing *AR* gain (in isolation) as a potential prognostic biomarker (Fig. 4B; Table 3; ref. 4). To determine whether there was a differential association with clinical outcomes depending on the degree of *AR* amplification, we calculated the average number of *AR* copies in the ctDNA component of each sample by adjusting *AR* coverage log ratios by estimated ctDNA%. With this approach, the median number of *AR* copies in samples exhibiting gain was 7.1 (highest 56). Patients with high *AR* gain (8+ copies) showed a trend for shorter TTP than patients with low *AR* gain (Fig. 4B), but significance was again not reached in multivariate analysis (Table 3). Consistent with these observations, although general *AR* gain was not more common in patients with TTP < 12 weeks (69% vs. 51% of patients with ctDNA > 2%, $P = 0.13$), high *AR* gain was detected in 43% of patients with ctDNA > 2% who exhibited primary resistance compared with only 18% of those who responded to therapy for more than 12 weeks ($P = 0.01$, Fisher exact test).

Missense mutations in the *AR* ligand-binding domain (LBD) were identified in 14 of 115 (12%) samples with ctDNA above detection thresholds and were found predominantly in patients without high *AR* gain (<8 copies; $P = 0.033$, Fisher exact test; Fig. 4A). The most common mutation was H875Y (nine patients). *AR* W742* mutations were detected in three patients, all of whom had received prior bicalutamide. No T878A or L702H mutations were detected at baseline. The absence of L702H is reflective of a cohort largely unexposed to supraphysiologic levels of corticosteroids. Patients with *AR* LBD mutations did not display shorter TTP even in univariate analysis (Table 3).

AR Gene Truncations in ctDNA Are Associated with Primary Resistance

Truncated AR variants with intact N-terminal domain and DNA binding domain (exons 1–3) can display ligand-independent activity (14). Although truncation of the LBD can occur through alternative splicing of cryptic exons (15), *AR* genomic structural rearrangements (*AR*-GSR) can also give rise to ligand-independent variants (16, 17). To assess the relevance of *AR*-GSRs for first-line abiraterone or enzalutamide response, we applied a sequencing approach designed

to capture *AR* introns in 50 patient samples with high ctDNA (median 43%, range, 12%–89%; Supplementary Fig. S15). Nineteen of 50 (38%) patient samples showed evidence for somatic *AR*-GSRs (Supplementary Figs. S16–S17; Supplementary Tables S8–S9). *AR*-GSRs were more common in samples with *AR* gain (46% vs. 9%, $P = 0.050$, Fisher exact test). Patients with truncating *AR*-GSRs downstream of exon 3 were more likely to have rising PSA as best response to therapy than patients with only non–LBD-truncating *AR*-GSRs (4/8 vs. 0/11; $P = 0.036$, Fisher exact test). Of the five patients with poorest PSA response to abiraterone/enzalutamide therapy, four carried truncating *AR*-GSRs downstream of exon 3 (Supplementary Fig. S16). Two more patients (126 and 168) with such *AR*-GSRs had rapid clinical progression (death within 3.2 and 4.7 months, respectively) despite an initial PSA response.

Only patient 058 carried an *AR* rearrangement in the absence of *AR* amplification: an 11.4-kb intragenic deletion from 23 bp downstream of exon 4 to within exon 7 (Fig. 4C). The deletion was detected by both the 72-gene sequencing panel and the *AR* panel. Using a PCR and Sanger sequencing approach applied to cDNA from patient 058's matched whole-blood RNA sample, we identified a unique *AR* transcript composed of exons 1 to 4, followed by 23 bp from the beginning of intron 4, followed by the last 70 bp of exon 7 and full exon 8 (Fig. 4C; Supplementary Fig. S16). The noncanonical junction between exons 4 and 7 resulted in a frameshift and premature stop codon 41 aa after the junction, truncating the AR protein before the LBD. In accordance with the absence of intact AR in his tumor cells, patient 058 displayed no response to abiraterone (83% PSA increase during first month; Fig. 4C).

DISCUSSION

Enzalutamide and abiraterone were developed to overcome reactivated AR signaling after clinical progression on standard hormonal therapies (18–20). Consistent with their strong activity in preclinical models of CRPC, we report that in patients unexposed to prior therapy for their mCRPC, enzalutamide and abiraterone elicit clinical responses in the context of *AR* amplifications and LBD mutations (specifically W742C and H875Y). Nevertheless, *AR* amplifications were associated with shorter TTP in univariate analyses, with a hazard ratio similar to that identified in a recent study leveraging droplet digital PCR to examine plasma cfDNA *AR* amplification status in first-line mCRPC (4). In our study, detection of *AR* amplification lost its prognostic effect after adjustment for routine prognostic clinical markers and ctDNA presence, diminishing its potential as an independent biomarker in first-line mCRPC. Pertinently, most of the poorest responders with *AR* gains were patients with high *AR* copy number (>8). This implies a dose effect for overcoming potent inhibition. A recent patient-derived tumor xenograft study demonstrated sequential ERK signaling inhibitor monotherapy selects for a progressively higher *BRAF* copy number that enables resistance (21). It is plausible that continuing evolution of *AR* copy number in mCRPC during first-line therapy contributes to cross-resistance between AR-targeted agents.

We detected diverse *AR*-GSRs, enriched in patients with additional *AR* copies. Specific *AR*-GSRs resulting in "hard-wired" ligand independence have been observed in model systems, but only recently in patients (17, 22). Although a prior study of 30 patients with heavily pretreated mCRPC suggested an association between detection of any *AR*-GSR and poor clinical response to AR-targeted therapy (22), the relevance for patients with treatment-naïve mCRPC remained unclear. In our study, only a subset of *AR*-GSRs appeared to have the potential to truncate the LBD without compromising the DNA binding and transactivation domains critical to AR protein function. Our data suggest that this *AR*-GSR subset contributes to primary resistance to first-line AR-targeted therapy in mCRPC. Previous studies have reported associations between truncated *AR* splice variants, particularly *ARV7*, and poor response to AR-targeted therapy (8, 9). However, most *ARV7*-positive patients also express high levels of full-length *AR*, and expression of *ARV7* in first-line mCRPC is rare and does not preclude response to AR-targeted therapy (9, 23). Given the diversity of *AR*-GSRs, and the potential impact of mRNA surveillance on their translation, it will be important to accurately identify the subset of *AR*-GSRs that genuinely lead to truncated AR proteins. We demonstrate that a novel *AR* transcript was robustly detected in matched whole blood from a patient with an LBD truncating *AR*-GSR. This suggests that whole blood or circulating tumor cell *AR* transcript profiling can help augment cfDNA screening for identification of clinically relevant *AR*-GSRs. Future studies are needed to assess the relative impact of *ARV7* and *AR*-GSRs on therapy response.

The association between homologous recombination repair (HRR) defects and primary resistance to AR-targeted therapy is consistent with reports of poor prognosis in this patient population (24). In a previous retrospective study we demonstrated a link between germline HRR defects and poor response to AR-targeted therapies (10). The current study represents a prospective validation and suggests that the association extends to somatic mutations in *BRCA2* and *ATM*. It is plausible that the increased tumor heterogeneity and adaptability enabled by a truncal DNA repair defect fosters the generation of clones with *de novo* resistance. Patients with mCRPC with HRR defects appear to benefit from treatment with PARP inhibitors or platinum-based chemotherapy (25, 26). Importantly, truncating mutations in *BRCA2*/*ATM* exhibited somatic LOH in all assessable cases, suggesting that accurate copy-number calling (often impossible at low ctDNA%) may not be an absolute requirement in guiding the use of these therapies. It should be noted however that there is a potential bias from examining only patients with a high tumor burden (i.e., those with high ctDNA fraction). Nevertheless, as liquid biopsies are also showing great promise in monitoring patients for reversion mutations linked to PARP inhibitor resistance (27, 28), they are likely to have broad clinical utility in patients with HRR-defective tumors. Future studies must assess the degree to which defects in other HRR genes (e.g., *CDK12*) are linked to poor outcomes with AR-directed therapies, but will require larger cohorts.

p53 and PI3K pathway defects were associated with poor response to AR-targeted therapy, with *TP53* defects retaining significance in multivariate models. This is consistent with data from experimental systems and human tissue studies suggesting that defects in *TP53* or *PI3K* reduce prostate cancer dependency on AR signaling (29–32). Complete *TP53* loss,

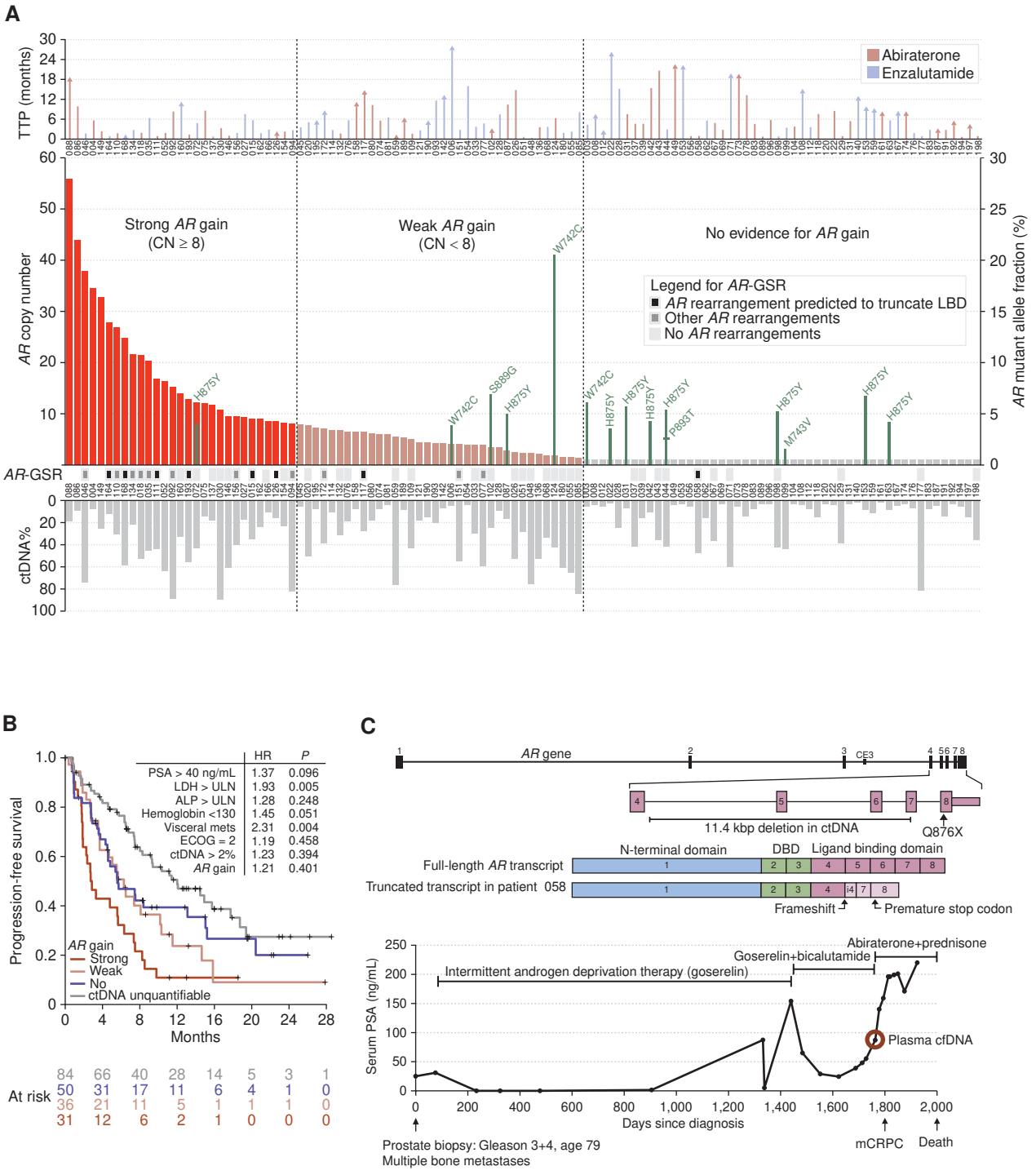

Figure 4. Effect of *AR* alterations on abiraterone/enzalutamide response. **A,** Bar plot showing estimated *AR* copy number (CN) in cancer cells (left y-axis). Patients were divided into three groups: high *AR* gain (more than 8 copies), low *AR* gain (detectable gain but less than 8 copies), and copy-neutral *AR*. *AR* mutations and their allele fractions are shown with green bars (right y-axis). TTP is shown at the top. Arrowheads indicate right-censored TTP. ctDNA% is shown at the bottom. **B,** Kaplan–Meier curves showing progression-free survival of patients with strong *AR* gain, weak *AR* gain, copy-neutral *AR* (but quantifiable ctDNA), and no quantifiable ctDNA. **C,** Example of somatic *AR*-GSR identified in patient 058. An 11.4-kbp deletion truncates the *AR* ligand binding domain. Timeline at bottom shows that patient 058 had no PSA response to abiraterone therapy and died soon after.

in conjunction with *RB1* loss, contributes to lineage plasticity and evolution toward an AR-negative state (31, 32). AR activity is reduced upon PTEN loss, and PI3K pathway activation can compensate for AR inhibition (29). The detection of PI3K defects in liquid biopsies offers opportunities for combining AR-targeted therapy with AKT/PI3K/mTOR inhibitors, because recent phase II data suggest patients with *PTEN* loss respond better to abiraterone plus AKT inhibition than abiraterone alone (33). Although our data do not propose that patients harboring *TP53* defects should entirely avoid AR-targeted therapy, we posit that the detection of a *TP53* defect has clinical utility: precipitating closer disease monitoring, preparing the patient for rapid progression, and encouraging the physician to ready future lines of therapy.

Our study reveals the relative impact of common genomic alterations on patient response to the most widely used therapies for advanced prostate cancer. Importantly, this work was performed within the framework of a large randomized phase II trial, leveraging minimally invasive liquid biopsies in a patient population representative of clinical practice. Key limitations include the exploratory nature of our analyses (in the absence of a prospective analysis plan) and the fact that we cannot put results in context of other prognostic biomarkers such as *ARV7* expression and CTC enumeration (9, 34). Furthermore, only 115 patients had sufficient ctDNA for genomic evaluation, which prevented us from assessing the clinical relevance of differing combinations of genomic alterations, and whether any specific combinations may be associated with complete lack of benefit from abiraterone or enzalutamide. Use of unique molecular identifiers and higher sequencing depths in the future will increase the proportion of patients with detectable ctDNA, but it is important to note that low ctDNA fraction was associated with good prognosis. Larger prospective randomized studies enrolling thousands of patients are required to address these questions and to validate potential predictive ctDNA biomarkers, but the results described here provide a crucial foundation for their design. Future studies must assess how these potential biomarkers generalize to castration-sensitive disease.

METHODS

Study Design and Patients

Two hundred two patients with treatment-naïve mCRPC who were eligible for treatment with abiraterone and enzalutamide were randomized 1:1 to a multicenter, phase II study of abiraterone and prednisone versus enzalutamide, with crossover at PSA progression. Approval for this study was granted by the University of British Columbia Research Ethics Board (Number H14-00738). The study was conducted in accordance with the Declaration of Helsinki, and written informed consent was obtained from all participants prior to enrollment. Patients received either abiraterone (1000 mg daily) + prednisone (5 mg twice daily) or enzalutamide (160 mg daily). Treatment continued until disease progression, death, or unacceptable toxicity. For the present analysis, we evaluated the following clinical endpoints with first-line therapy: PSA decline ≥ 50% (PSA50) from baseline, time to PSA progression with first-line therapy, and TTP [defined as first of confirmed PSA progression (Prostate Cancer Clinical Trials Working Group 3), clinical or radiologic progression, or death from disease]. A prespecified secondary objective of this trial was the identification of potential plasma-based biomarkers that are associated with treatment efficacy and/or resistance among patients with mCRPC receiving abiraterone acetate and enzalutamide.

Target Capture and Sequencing

A custom NimbleGen SeqCap EZ Choice target capture panel was used to capture the coding regions of 72 genes (Supplementary Table S2). For each sample, 10 to 100 ng of DNA was used for library preparation. All germline DNA samples were sheared into 180-bp fragments with a Covaris focused ultrasonicator. A-tailing, end-repair, Illumina-compatible adapter ligation and PCR amplification (between 12 and 17 cycles) was performed. Library quantification was carried out with the NanoDrop spectrophotometer, and each library was run on an ethidium bromide gel to confirm success. Up to 25 purified sample libraries at a time were multiplexed to obtain single pools with a combined mass of 1 μg, allowing a minimum 40 ng input for each sample library. These pools were hybridized to the capture panel for a minimum of 16 hours at 47°C. The subsequent wash, recovery, and amplification of the captured regions were performed according to the NimbleGen SeqCap EZ system protocols. Final libraries were purified with Agencourt AMPure beads and quantitated using either the KAPA qPCR kit, or the Qubit 2.0 Fluorometer (Life Technologies) and Qubit dsDNA HS Assay Kit. Pools were diluted to 20 pmol/L and were sequenced on Illumina MiSeq (V3 600 cycle kit) or HiSeq 2500 (V4 250 cycle kit) machines. Exome capture and sequencing was performed using libraries previously prepared for targeted sequencing, and following the identical protocols described above, utilizing the Roche Nimblegen SeqCap EZ MedExome kit. Sequencing data have been deposited to the European Genome–phenome Archive (EGA) under accession EGAS00001003113 (as patients PC-001 to PC-202).

Sequence Alignment and Quality Control

Paired-end reads were aligned against the hg38 reference genome using Bowtie-2.3.0 (35). Optical and PCR duplicates were removed using samblaster 0.1.24 (36). Adapters were trimmed in paired mode using cutadapt 1.11 (37). Low-quality read tails (smoothed baseq <30) were trimmed using an in-house algorithm. Per-base read coverages in target regions were counted using bedtools 2.25.0 (38). cfDNA/white blood cell (WBC) sample pairings were verified based on SNP genotypes.

Analysis of Somatic Mutations

Somatic mutations were called in cfDNA samples by searching for variants with an alternate allele fraction of at least 1% and at least 10 supporting reads. Additionally, the allele fraction was required to be 25 times higher than the background error rate (i.e., the average allele fraction across all WBC samples), and 3 times higher than the allele fraction in the paired WBC sample. The paired WBC sample was required to have at least 20 reads covering the site. Protein-level consequences of variants were predicted using ANNOVAR (39).

Analysis of Germline Variants

Germline variants were called in WBC samples by searching for variants with an alternate allele fraction of at least 15% and at least 5 supporting reads. Germline variants with a population allele frequency of 0.5% or higher in the KAVIAR or ExAC databases were ignored. Protein-level consequences of variants were predicted using ANNOVAR (39).

Estimation of ctDNA Fraction

ctDNA fractions (ctDNA%) were estimated based on the allele fractions of autosomal somatic mutations. We first observed that the mutant allele fraction (MAF) in diploid chromosomes is highest when the mutation is combined with LOH (somatic mutations in genes with a detectable amplification were ignored in ctDNA% estimation). In this situation, the MAF and ctDNA% are related as

MAF = (ctDNA × 1)/[(1 − ctDNA) × 2 + ctDNA × 1], and so ctDNA = 2/(1/MAF + 1). Because deletions and LOH are not detectable from low ctDNA fractions, we conservatively assumed that all mutations could have associated LOH. To deal with stochastic variation in observed mutant allele read counts, we modeled the mutant read count as arising from a binomial distribution, and conservatively calculated what the true MAF would be if the highest observed MAF was a 95% quantile outlier.

Copy-Number Calling

Reads were counted in all capture regions using bedtools 2.25.0 (38). Coverage log ratios were calculated against a median reference derived from all WBC samples. Guanine-cytosine (GC) fraction was calculated for all target regions, and Loess regression was applied to bait log ratios to correct for GC content bias. After GC bias correction, read counts were corrected for residual differences in overall coverage using median-of-ratios normalization.

Because hemizygous copy-number changes are associated with a loss of one allele at heterozygous bases, we used WBC samples to find all heterozygous germline SNPs in captured regions, and then calculated the allele fractions of those SNPs in the corresponding cfDNA samples. We then calculated a median divergence from heterozygosity, defined as median [abs(AF − 0.5)], for each gene and cfDNA sample.

A deletion was called for a gene when coverage log ratio ≤ −0.1 and MAF ≥ 0.6, or regardless of MAF if coverage log ratio ≤ −0.3. A gain was called for a gene when coverage log ratio ≥ 0.1 and MAF ≥ 0.6, or regardless of MAF if log ratio ≥ 0.3. These conservative thresholds were determined empirically by studying a plot of coverage log ratios and heterozygous SNP allele fractions in samples with and without detectable ctDNA (Supplementary Fig. S14).

ctDNA fraction–corrected absolute *AR* copy numbers were estimated using the formula $C_{abs} = (2^L - 1)/F + 1$, where C_{abs} is the absolute copy number, L is the read coverage log ratio inside the gene, and F is the ctDNA fraction. cfDNA samples showing evidence for *AR* gain were dichotomized into low and high AR gain subgroups, using eight absolute AR copies (the median) as the threshold.

Analysis of Somatic Genomic Rearrangements

Unaligned reads from each sample were split into two 30-bp anchors (from the 5′ and 3′ ends of the read) and aligned to the hg38 genome. Discordant anchor pairs were grouped by position and breakpoint signature. Duplicate reads arising from the same original cfDNA fragment (or from PCR/optical duplicates of the same original cfDNA fragment) were discarded based on read IDs and read start positions. Rearrangement candidates supported by three or more unique cfDNA fragments were manually curated using IGV and BLAT.

Identification of Truncated AR Transcripts from Whole Blood

All patients were subjected to a peripheral blood (2.5 mL) collection in a PAXgene RNA tube, matched to the time of baseline plasma cfDNA collection. This system has previously been used for the discovery of whole-blood RNA gene expression profiles that correlate with mCRPC prognoses, as well as for determining presence or absence of the truncated *AR* splice variant *ARV7* (40–42). Tubes were stored at −80°C. We thawed blood overnight and extracted RNA using the PAXgene blood RNA kit. Reverse transcription was performed with the SuperScript II enzyme using 10 μL of total RNA. We used a standard PCR and Sanger sequencing approach with primers designed flanking the rearrangement.

Statistical Framework for Survival Analysis

For each clinical and genomic variable, hazard ratios and *P* values were calculated using Cox proportional hazards models, as implemented in the "survival" package (version 2.41.3) for the R programming language (version 3.4.0). We assessed the independent biomarker potential of each genomic alteration by constructing multivariate Cox proportional hazards models assessing each individual alteration (positive vs. negative) together with baseline ctDNA% (dichotomized at 2%), baseline LDH [dichotomized at upper limit of normal (ULN)], baseline ALP (dichotomized at ULN), presence of visceral metastases, baseline PSA (dichotomized at 40 ng/mL), hemoglobin (dichotomized at 130 g/L), and high Eastern Cooperative Oncology Group performance status (2 vs. 0–1) as binary covariates. Patients' age (dichotomized at 75 years) was excluded from multivariate models as it did not reach significance in univariate analysis (Table 2). Additionally, to test whether the prognostic effect of a given genomic alteration was independent of all other detected alterations, we constructed a single multivariate Cox proportional hazards model including all genomic variables together with the clinical prognostic factors described above. The statistical framework is illustrated in Supplementary Fig. S18.

Disclosure of Potential Conflicts of Interest

C. Kollmannsberger is a consultant/advisory board member for Pfizer, BMS, Ipsen, Astellas, Bayer, and Merck. D. Finch has received honoraria from the speakers bureaus of Janssen and Astellas and is a consultant/advisory board member for Janssen and Astellas. A.A. Azad reports receiving a commercial research grant from Astellas, has received honoraria from the speakers bureaus of Astellas and Janssen, and is a consultant/advisory board member for Astellas and Janssen. K.N. Chi reports receiving commercial research grants from Janssen and Astellas and is a consultant/advisory board member for Janssen and Astellas. No potential conflicts of interest were disclosed by the other authors.

Authors' Contributions

Conception and design: C. Kollmannsberger, A.A. Azad, M.E. Gleave, A.W. Wyatt, K.N. Chi

Development of methodology: M. Annala, A.A. Azad, A.W. Wyatt, K.N. Chi

Acquisition of data (provided animals, acquired and managed patients, provided facilities, etc.): G. Vandekerkhove, D. Khalaf, K. Beja, E.W. Warner, C. Kollmannsberger, B.J. Eigl, D. Finch, C.D. Oja, J. Vergidis, M. Zulfiqar, A.A. Azad, M.E. Gleave, K.N. Chi

Analysis and interpretation of data (e.g., statistical analysis, biostatistics, computational analysis): M. Annala, G. Vandekerkhove, S. Taavitsainen, K. Sunderland, C. Kollmannsberger, A.W. Wyatt, K.N. Chi

Writing, review, and/or revision of the manuscript: M. Annala, G. Vandekerkhove, K. Sunderland, C. Kollmannsberger, B.J. Eigl, M. Zulfiqar, M.E. Gleave, A.W. Wyatt, K.N. Chi

Administrative, technical, or material support (i.e., reporting or organizing data, constructing databases): D. Khalaf, K. Beja, E.W. Warner, K. Sunderland, M. Zulfiqar

Study supervision: C.D. Oja, M. Zulfiqar, M. Nykter, A.W. Wyatt, K.N. Chi

Acknowledgments

This work was supported by CCSRI Innovation Grant #702837 (K.N. Chi and A.W. Wyatt), Prostate Cancer Canada through Movember Discovery Grants #D2015-06 (A.W. Wyatt and K.N. Chi) and #D2014-13 (K.N. Chi and A.W. Wyatt) and the Movember Rising Star in Prostate Cancer research program (A.W. Wyatt), the Emil Aaltonen Foundation (M. Annala), the Prostate Cancer Foundation (A.W. Wyatt and K.N. Chi), Terry Fox New Frontiers Program Project grant #TFF116129 (M.E. Gleave, A.W. Wyatt, and K.N. Chi), and clinical trials funding from Janssen and Astellas. The study funders had no role in the design of the study; the collection, analysis, and interpretation of the data; the writing of the manuscript; or the decision to

submit the manuscript for publication. We thank Lejla Gavranovic and Leanne Chiu (clinical coordinators) as well as Kelly Halvorsen and Nikita Ivanov (research nurses).

Received August 17, 2017; revised October 19, 2017; accepted January 18, 2018; published first January 25, 2018.

REFERENCES

1. Beer TM, Armstrong AJ, Rathkopf DE, Yohann L, Sternberg CN, Higano CS, et al. Enzalutamide in metastatic prostate cancer before chemotherapy. N Engl J Med 2014;371:424–33.
2. Ryan CJ, Smith MR, de Bono JS, Arturo M, Logothetis CJ, de Souza P, et al. Abiraterone in metastatic prostate cancer without previous chemotherapy. N Engl J Med 2013;368:138–48.
3. Romanel A, Tandefelt DG, Conteduca V, Jayaram A, Casiraghi N, Wetterskog D, et al. Plasma AR and abiraterone-resistant prostate cancer. Sci Transl Med 2015;7:312re10–312re10.
4. Conteduca V, Wetterskog D, Sharabiani MTA, Grande E, Fernandez-Perez MP, Jayaram A, et al. Androgen receptor gene status in plasma DNA associates with worse outcome on enzalutamide or abiraterone for castration-resistant prostate cancer: a multi-institution correlative biomarker study. Ann Oncol 2017;28:1508–16.
5. Wyatt AW, Azad AA, Volik SV, Annala M, Beja K, McConeghy B, et al. Genomic alterations in cell-free DNA and enzalutamide resistance in castration-resistant prostate cancer. JAMA Oncol 2016;2:1598–606.
6. Ulz P, Belic J, Graf R, Auer M, Lafer I, Fischereder K, et al. Whole-genome plasma sequencing reveals focal amplifications as a driving force in metastatic prostate cancer. Nat Commun 2016;7:12008.
7. Azad AA, Volik SV, Wyatt AW, Haegert A, Le Bihan S, Bell RH, et al. Androgen receptor gene aberrations in circulating cell-free DNA: biomarkers of therapeutic resistance in castration-resistant prostate cancer. Clin Cancer Res 2015;21:2315–24.
8. Antonarakis ES, Lu C, Wang H, Luber B, Nakazawa M, Roeser JC, et al. AR-V7 and resistance to enzalutamide and abiraterone in prostate cancer. N Engl J Med 2014;371:1028–38.
9. Scher HI, Lu D, Schreiber NA, Louw J, Graf RP, Vargas HA, et al. Association of AR-V7 on circulating tumor cells as a treatment-specific biomarker with outcomes and survival in castration-resistant prostate cancer. JAMA Oncol 2016;2:1441–9.
10. Annala M, Struss WJ, Warner EW, Beja K, Vandekerkhove G, Wong A, et al. Treatment outcomes and tumor loss of heterozygosity in germline DNA repair-deficient prostate cancer. Eur Urol 2017;72:34–42.
11. Wyatt AW, Annala M, Aggarwal R, Beja K, Feng F, Youngren J, et al. Concordance of circulating tumor DNA and matched metastatic tissue biopsy in prostate cancer. J Natl Cancer Inst 2017;109.
12. Robinson D, Van Allen EM, Wu Y-M, Schultz N, Lonigro RJ, Mosquera J-M, et al. Integrative clinical genomics of advanced prostate cancer. Cell 2015;161:1215–28.
13. Grasso CS, Wu Y-M, Robinson DR, Cao X, Dhanasekaran SM, Khan AP, et al. The mutational landscape of lethal castration-resistant prostate cancer. Nature 2012;487:239–43.
14. Ho Y, Dehm SM. Androgen receptor rearrangement and splicing variants in resistance to endocrine therapies in prostate cancer. Endocrinology 2017;158:1533–42.
15. Hu R, Dunn TA, Wei S, Isharwal S, Veltri RW, Humphreys E, et al. Ligand-independent androgen receptor variants derived from splicing of cryptic exons signify hormone-refractory prostate cancer. Cancer Res 2009;69:16–22.
16. Li Y, Chan SC, Brand LJ, Hwang TH, Silverstein KAT, Dehm SM. Androgen receptor splice variants mediate enzalutamide resistance in castration-resistant prostate cancer cell lines. Cancer Res 2013;73:483–9.
17. Henzler C, Li Y, Yang R, McBride T, Ho Y, Sprenger C, et al. Truncation and constitutive activation of the androgen receptor by diverse genomic rearrangements in prostate cancer. Nat Commun 2016;7:13668.
18. Chen CD, Welsbie DS, Tran C, Baek SH, Chen R, Vessella R, et al. Molecular determinants of resistance to antiandrogen therapy. Nat Med 2004;10:33–9.
19. Tran C, Ouk S, Clegg NJ, Chen Y, Watson PA, Arora V, et al. Development of a second-generation antiandrogen for treatment of advanced prostate cancer. Science 2009;324:787–90.
20. Attard G, Belldegrun AS, de Bono JS. Selective blockade of androgenic steroid synthesis by novel lyase inhibitors as a therapeutic strategy for treating metastatic prostate cancer. BJU Int 2005;96:1241–6.
21. Xue Y, Martelotto L, Baslan T, Vides A, Solomon M, Mai TT, et al. An approach to suppress the evolution of resistance in BRAFV600E-mutant cancer. Nat Med 2017;23:929–37.
22. De Laere B, van Dam P-J, Whitington T, Mayrhofer M, Diaz EH, Van den Eynden G, et al. Comprehensive profiling of the androgen receptor in liquid biopsies from castration-resistant prostate cancer reveals novel intra-AR structural variation and splice variant expression patterns. Eur Urol 2017;72:192–200.
23. Bernemann C, Schnoeller TJ, Luedeke M, Steinestel K, Boegemann M, Schrader AJ, et al. Expression of AR-V7 in circulating tumour cells does not preclude response to next generation androgen deprivation therapy in patients with castration resistant prostate cancer. Eur Urol 2017;71:1–3.
24. Castro E, Goh C, Olmos D, Saunders E, Leongamornlert D, Tymrakiewicz M, et al. Germline BRCA mutations are associated with higher risk of nodal involvement, distant metastasis, and poor survival outcomes in prostate cancer. J Clin Oncol 2013;31:1748–57.
25. Mateo J, Carreira S, Sandhu S, Miranda S, Mossop H, Perez-Lopez R, et al. DNA-repair defects and olaparib in metastatic prostate cancer. N Engl J Med 2015;373:1697–708.
26. Cheng HH, Pritchard CC, Boyd T, Nelson PS, Montgomery B. Biallelic inactivation of BRCA2 in platinum-sensitive metastatic castration-resistant prostate cancer. Eur Urol 2016;69:992–5.
27. Goodall J, Mateo J, Yuan W, Mossop H, Porta N, Miranda S, et al. Circulating Free DNA to guide prostate cancer treatment with PARP inhibition. Cancer Discov 2017;7:1006–17.
28. Quigley D, Alumkal JJ, Wyatt AW, Kothari V, Foye A, Lloyd P, et al. Analysis of circulating cell-free DNA identifies multi-clonal heterogeneity of BRCA2 reversion mutations associated with resistance to PARP inhibitors. Cancer Discov 2017;7:999–1005.
29. Carver BS, Chapinski C, Wongvipat J, Hieronymus H, Chen Y, Chandarlapaty S, et al. Reciprocal feedback regulation of PI3K and androgen receptor signaling in PTEN-deficient prostate cancer. Cancer Cell 2011;19:575–86.
30. Beltran H, Prandi D, Mosquera JM, Benelli M, Puca L, Cyrta J, et al. Divergent clonal evolution of castration-resistant neuroendocrine prostate cancer. Nat Med 2016;22:298–305.
31. Mu P, Zhang Z, Benelli M, Karthaus WR, Hoover E, Chen C-C, et al. SOX2 promotes lineage plasticity and antiandrogen resistance in TP53- and RB1-deficient prostate cancer. Science 2017;355:84–8.
32. Ku SY, Rosario S, Wang Y, Mu P, Seshadri M, Goodrich ZW, et al. Rb1 and Trp53 cooperate to suppress prostate cancer lineage plasticity, metastasis, and antiandrogen resistance. Science 2017;355:78–83.
33. de Bono JS, De Giorgi U, Massard C, Bracarda S, Nava Rodrigues D, Kocak I, et al. PTEN loss as a predictive biomarker for the Akt inhibitor ipatasertib combined with abiraterone acetate in patients with metastatic castration-resistant prostate cancer (mCRPC). Ann Oncol 2016;27:7180
34. Scher HI, Heller G, Molina A, Attard G, Danilla DC, Jia X, et al. Circulating tumor cell biomarker panel as an individual-level surrogate for survival in metastatic castration-resistant prostate cancer. J Clin Oncol 2015;33:1348–55
35. Langmead B, Salzberg SL. Fast gapped-read alignment with Bowtie 2. Nat Methods 2012;9:357–9.

36. Faust GG, Hall IM. SAMBLASTER: fast duplicate marking and structural variant read extraction. Bioinformatics 2014;30:2503–5.
37. Martin M. Cutadapt removes adapter sequences from high-throughput sequencing reads. EMBnet.J 2011;17:10–2.
38. Quinlan AR, Hall IM. BEDTools: a flexible suite of utilities for comparing genomic features. Bioinformatics 2010;26:841–2.
39. Wang K, Li M, Hakonarson H. ANNOVAR: functional annotation of genetic variants from high-throughput sequencing data. Nucleic Acids Res 2010;38:e164.
40. Olmos D, Brewer D, Clark J, Danila DC, Parker C, Attard G, et al. Prognostic value of blood mRNA expression signatures in castration-resistant prostate cancer: a prospective, two-stage study. Lancet Oncol 2012;13:1114–24.
41. Danila DC, Anand A, Schultz N, Heller G, Wan M, Sung CC, et al. Analytic and clinical validation of a prostate cancer-enhanced messenger RNA detection assay in whole blood as a prognostic biomarker for survival. Eur Urol 2014;65:1191–7.
42. Todenhöfer T, Azad A, Stewart C, Gao J, Eigl BJ, Gleave ME, et al. AR-V7 transcripts in whole blood RNA of patients with metastatic castration resistant prostate cancer correlate with response to abiraterone acetate. J Urol 2017;197:135–42.